Scalable Nanopillar Arrays with Layer-by-Layer Patterned Overt and Covert Images

Kyoung G. Lee, Bong Gill Choi, Byeong Il Kim, Terry Shyu, Myung Seok Oh, Sung Gap Im, Sung-Jin Chang, Tae Jae Lee, Nicholas A. Kotov, and Seok Jae Lee**

Surface nanoscale features with an aspect ratio $r > 1$ (height/width) strongly affect the adhesion, charge and heat transfer, light scattering, tribology, liquid flow, wetting, cellular interactions, and many other processes at their interfaces.[1–3] Realizing these effects in nanopillar arrays (NPAs) can be a convenient tool for engineering the electrical, mechanical, and optical properties for flexible/wearable electronics,[4,5] energy storage devices, solar cells, biosensors,[6] dry adhesives,[7] and other applications.[8] NPAs made from polymers are particularly attractive compared to silicon, ZnO, and carbon nanotube NPAs because of the brittleness and opaqueness. Considerable exploratory investigations need to be carried out before polymeric NPAs can be produced in a scalable format that would enable the practical realization of their unique properties. The same is true for the preparation of polymeric NPAs on practical every-day substrates such as papers, textiles, and metals.

Soft lithography based on poly(dimethylsiloxane) (PDMS) elastomers has emerged as a promising approach for producing micro- and nanoscale surface features including NPAs.[9–12] Although PDMS has enabled fundamental advances in this area it is not an ideal material for constructing nanopillars. The same properties that render PDMS NPAs useful for studies of enhanced adhesion and tribology[3,13] also hinder their large-scale production. This is because nanopillars with a high aspect ratio are easily torn off from the substrate due to the strong adhesion forces between the NP and its mold. The poor mechanical strength of PDMS and its high affinity to silicon oxide surfaces have obstructed its successful, single-step detachment from templates. Consequently, a staged process with multiple lithography cycles, adding a sequence of thin strata to growing nanopillars – similar to constructing a multilevel building – has been developed to make nanoscale features.[14] This is a powerful technique that can afford complex 3D structures,[15] however, this technique comes at the expense of both excessive time and low yield. Furthermore, the successful transfer of sculpted PDMS onto other substrates in a continuous fashion, is difficult because of the low/high adhesion dilemma. On one hand, PDMS adhesion to non-silicon-based materials (other plastics, fabric, metal foil, etc.) is low whereas all the applications require it to be high. On the other hand, PDMS adhesion to the silicon template is high;[16] stresses generated during the template-removal process cause the detachment of the PDMS NPAs from these substrates even after in-situ polymerization of the PDMS precursors as demonstrated in Figure S1 (Supporting Information).

The lessons learned from NPAs from PDMS, ZnO, silicon, and carbon nanotubes[17] indicate the need for an alternative polymeric material that 1) improves the adhesion between the polymer and the target substrate, 2) reduces adhesion to the template, and 3) provides a scalable production of NPAs. Here, we demonstrate that it is possible and manufacture large-area NPAs over in a single-step replication process for a wide variety of substrates. A special polymeric blend containing polyurethane acrylate (PU) and NOA63 adhesive denoted here as PUNO, see Supporting Information, allows us to balance the conflicting requirements for a scalable, single-step replication process. This blend makes possible to make replica sheets from wafers as large as eight inches in diameter. Concomitantly, the PUNO-based NPAs can be easily transferred onto a range of substrates that we have tested.[18,19] The signature strength and toughness of the PUNO nanopillars is revealed in the flexible and shear-resilient surfaces capable of withstanding harsh mechanical conditions. Furthermore, the prepared NPAs are convenient substrates for surface modification using inkjet layer-by-layer deposition (LBL) that enables us to create hidden images based on controlled wetting behavior.

The nanopillars were initially produced on Si wafers by standard photolithography followed by dry etching (Experimental Section, **Figure 1**a and Supporting Information, S2). The Si

Dr. K. G. Lee,[†] Dr. B. G. Choi,[†] T. Shyu, Prof. N. A. Kotov
Department of Chemical Engineering
University of Michigan
Ann Arbor, Michigan 48109, USA
E-mail: kotov@umich.edu
Dr. K. G. Lee, Dr. B. I. Kim,[†] Dr. T. J. Lee, Dr. S. J. Lee
Department of Nano Bio Research
National Nanofab Center (NNFC)
Daejeon 305–806, Republic of Korea
E-mail: sjlee@nnfc.re.kr
Dr. B. G. Choi
Department of Chemical Engineering
Kangwon National University
Samcheok 245–711, Republic of Korea
M. S. Oh, Prof. S. G. Im
Department of Chemical & Biomolecular Engineering
Korea Advanced Institute of Science and Technology (KAIST)
Daejeon 305–701, Republic of Korea
Dr. S.-J. Chang
Division of Materials Science
Korea Basic Science Institute
Daejeon, Republic of Korea

[†]These authors contributed equally to this work.

DOI: 10.1002/adma.201401246

ADVANCED MATERIALS
www.advmat.de

Materials Views
www.MaterialsViews.com

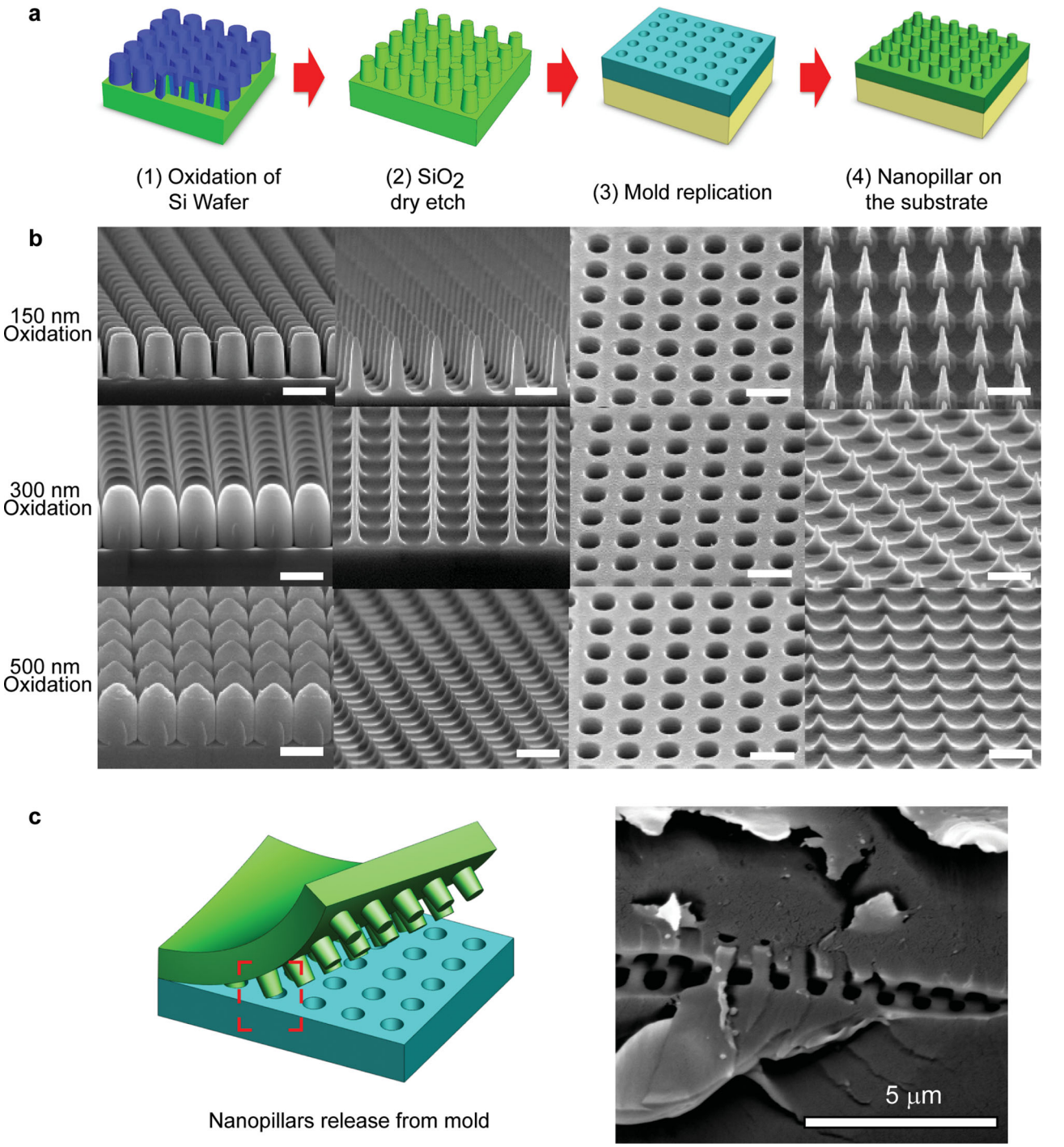

Figure 1. a) Schematic layout of the Si master-template formation and double replication to construct nanopillars on the target substrate. b) SEM images of different Si oxidation states (leftmost) and etching of SiO_2 to control the final dimensions of the nanopillars (rightmost). All the scale bars are 1 μm. c) Schematic illustration of nanopillar release from the mold and d) SEM image of the cross-section between the nanopillars and the mold displaying spontaneous detachment of the nanopillars from the mold walls after curing.

NPAs had cylindrical shapes with diameters of 500 nm and heights of 740 nm (Figure 1). In order to reduce the diameter of the pillars to increase the aspect ratio, we employed thermal oxidation and etching steps (Figure 1a and S3, Supporting Information). Three different thermal oxidation conditions were applied to form SiO_2 layers of different thicknesses (Figure 1b). Oxygen penetration into Si resulted in increased nanopillar diameters and a reduction of *r*, which seems to be counter-productive in the context of this study. However, the subsequent dry etching removed the SiO_2 layer and revealed nanopillars

with diameters as small as 50 nm, which is the smallest diameter reported to date (Figure S4, Supporting Information).[20]

Previously, we have observed that polymerization shrinkage commonly occurred with polymers impregnating silicon templates during the UV-curing process.[21,22] Being guided by these observations, we selected the composition of PU:NOA63 as 7:3 (v/v) because it demonstrated some but not extensive polymerization shrinkage. We hypothesized that this would help us to release the polymeric replica from the mold. The different ratios of PU and NOA63 were tested and the results are presented in Figure S5 in the Supporting Information. The UV-induced shrinking by about 1.3% (from SEM measurements) resulted in the detachment of the nanopillars from the walls of the mold (Figure 1c and 1d). Indeed, the adhesion of the polymer to the template was drastically lowered and a large sheet of cured PUNO can be easily peeled off as a flexible, patterned sheet. Note that besides spontaneous separation from the template this was also possible because PUNO displayed excellent mechanical properties with $E = 24$ MPa and $\sigma_{ult} = 11.5$ MPa (Figure S6, Supporting Information). In contrast, PDMS polymers typically show $E < 10$ MPa and $\sigma_{ult} < 2.4$ MPa. Consequently, PDMS-based nanopillars break when being detached from the substrate; consequently, single-step patterned surface features on PDMS are not possible.[22–25]

Due to the improved mechanical performance and greatly facilitated detachment process, the first replica from lithographically patterned substrates (Figure 1) displayed a uniform array of holes with nearly ideal fidelity over the entire surface (Figure 1). A similar cast-lift process can then be carried out using this hole-array as a template. The newly deposited liquid polymeric blend completely penetrates the mesoscale holes. Exposure to UV light results again in the detachment of the cured polymer from the walls of the wells and a replica of the original nanopillar array is formed. Both the original Si nanopillar and the PUNO hole mold are reusable.

Addition of NOA63 also allows us to resolve the problem of low adhesion to everyday substrates; in fact, it was exceptionally strong for PUNO. As a demonstration of such adhesion, a PET)/PUNO/PET composite film was stretched to failure, which required $\varepsilon = 321\%$ of strain (Figure S7a, Supporting Information). By contrast, the PDMS film was easily peeled off from the PET surface at the onset of sample testing (Figure S7b, Supporting Information) with strains $\varepsilon < 66\%$. From the stress–strain curve and the areas of PET-PUNO contact, we calculated the adhesion energy at the PUNO-PET interface to be 10.3 MPa, which compares favorably to that of 8.4 MPa of commercial superglue (DP8010, 3M).[26]

To gain insight into the interfacial interactions between the PUNO and the substrates, the Raman peak-intensity changes (2928 cm^{-1}) and peak-frequency shift (1617 cm^{-1}) were measured at the cross-section of the PUNO/fabric interfaces (**Figure 2**a–c) (Supporting Information). The Raman scattering peaks at 2928 cm^{-1} and 1617 cm^{-1} attributed to the ν_{C-H} stretch of PUNO and $\nu_{C=C}$ stretch of the aromatic ring of the polyester fabric, respectively, changed when PUNO was contacting the substrate (Figure 2b-d).[27] Furthermore, the strong red-shift of the Raman signal intensity for the peaks representing the hydrogen bonds (ν_{C-H}) in neat PUNO could also easily be observed at the interface after polymerization. The significant frequency shift that corresponds to the $\nu_{C=C}$ stretch of the aromatic rings from both PUNO and the polyester fabric indicated strong C=C bonds at the interface of the PUNO/fabric (Figure 2c). These observations indicate that both hydrogen bonds (ν_{C-H}) and other bonds associated with the easily

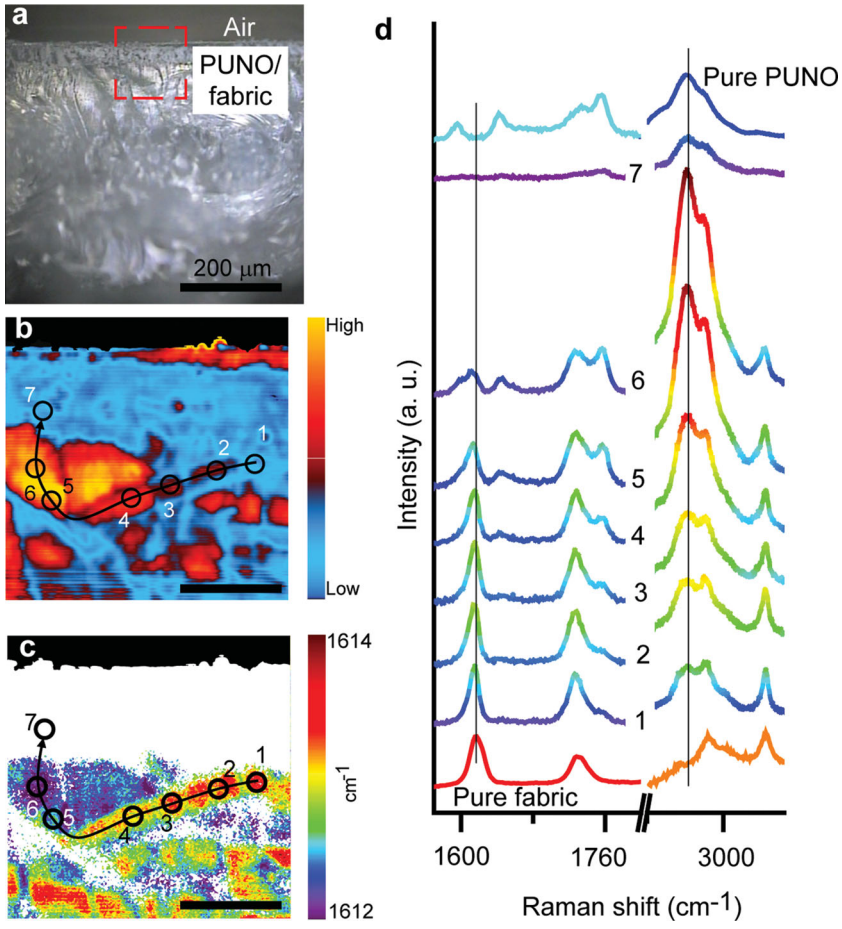

Figure 2. Raman spectroscopy of the interface between PUNO and the fabric. All Raman spectra were measured from the top of the cross-section of the sample along the line (1–7) with a 473 nm laser and 10x objective lens, which allowed both the pure PUNO and PUNO/fabric mixture to be measured. Note that the size of the laser beam at the cross-section was approximately 1.2 μm. a) Optical microscopy image of the cross-section of a PUNO/fabric composite film. b,c) Raman maps for b) the peak intensity at around 2928 cm^{-1} attributed to the ν_{C-H} stretch of PUNO and c) the peak frequency shift at around 1617 cm^{-1} attributed to the $\nu_{C=C}$ stretch of the aromatic ring of the fabric according to the red rectangular in (a). d) Raman spectra of neat PUNO, fabric, and the PUNO/fabric interface along the direction of the numbers in (b,c). The scale bars in (b) and (c) are 50 μm.

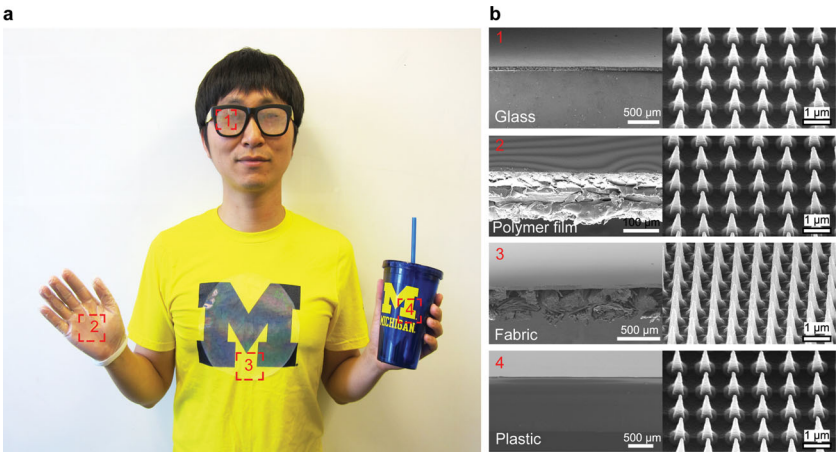

Figure 3. a) Photographic image of nanopillars on diverse substrates, including glasses (1), a polymeric glove (2), a T-shirt (3), and a plastic cup (4). b) SEM images showing the cross-section of the boundary and the surface of the nanopillar arrays on the corresponding materials in image (a).

polarizable C=C bonds are likely to be involved in the attachment of PUNO to the fabrics.

To demonstrate integration of our NPAs with typical household items and goods, we selected a polymer glove, a T-shirt, a plastic cup, glasses, paper, and aluminum foil as example materials (**Figure 3**a and S8, Supporting Information). We investigated whether successful bonding and replication of nanopillar arrays on the various substrates could take place without causing structural damage. SEM images were taken of both the cross section and the surface as seen in Figure 3b and S8 (Supporting Information). It is difficult to distinguish the boundary between the PUNO and the substrates because of its strong adhesion to the surfaces. Notably the resulting nanopatterned films display rainbow colors and opalescence because of the optical bandgap effect. When materials are covered with PUNO NPAs, one can see the logos and material colors through the thin film on the substrates, Figure 3a. As we can see later in the paper, this ability opens the door for a number of new applications of NPAs.

The mechanical properties of PUNO also come into play when NPAs from this material are subjected to shear strain. Notably, NPAs from other materials – PDMS, Si, SiO_2, and ZnO[27,28] are often easily rubbed off from the substrate. To investigate the rubbing resistance of our NPAs from PUNO we decided to use the superhydrophobic form of the nanopillars. The high contact angle (CA) with water is convenient for testing the shear resilience on the substrates. The superhydrophobic NPAs were produced by surface modification with poly(3,3,4,4,5,5,6,6,7,7,8,8,9,9,10,10,10-heptadecafluorodecyl methacrylate) in an initiated chemical vapor deposition (iCVD) method (Figure S8a and S9 in the Supporting Information). Alternatively, superhydrophilic surfaces could be produced by sputtering a SiO_2 layer on the top (ca. 5 nm) (Figure S9b, S10, and S11, Supporting Information). The overall CA changes with the NAP morphology and the surface modification is apparent in **Figure 4**a. We rubbed the superhydrophobic NPA film (Figure 4b) with different materials such as cloth, a brush, and a finger more than 500 times under a pressure of 4.9 KPa (Figure 4c and Figure S12, Supporting Information). The initial CA was 159° ± 0.39, which gradually decreased to 138° ± 5.9 (Figure 4d). The pillars were bent along the force direction but the overall structures were remained over the substrate. Furthermore, the ability to repel water droplets was retained (Movie S1 and S2 in the Supporting Information). In comparison, the previously reported superhydrophobic films became hydrophilic with a CA = 45° ± 8 within 5 rubs with the same pressure.[28,29]

We also combined NPAs and layer-by-layer assembly (LBL) by depositing multiple conformal hydrophilic layers on top of the hydrophobic pillars using inkjet LBL modality[30] (**Figure 5** and Movie S3, Supporting Information). This finding opens the way to highly customizable images on a variety of substrates. The nanometer-scale thick LBL coating does not change the appearance of the nanopillars or their periodicity and therefore it remains virtually invisible (Figure 5a). However, it strongly changes the local CA, which enabled us to create inkjet-printable hidden images. These are only revealed by exposure to a change in relative humidity, for instance, by breathing on them (Figure 5b). As the LBL layer becomes thicker and the space between the nanopillars becomes more filled, highly visible images can be printed as well (Figure 5d,e). The combination of overt and covert information can be applicable as anti-counterfeit tags. Human-breath visualization can be a simple method of authentication that is applicable to most products currently being counterfeited.

In conclusion, balancing the adhesion and mechanical strength of the curable polymer matrix allowed us to develop a new method of NPA production that is scalable and universally adhesive on various substrates. It can be accomplished by using a special polyurethane blend that enables their single-step replication with high fidelity. Moreover, the technique affords the transfer of NPA onto a variety of substrates, including fabric, paper, and metals via intermolecular bonds. The NPA maintains its structure, flexibility, and wettability even after rubbing with various materials, including a finger, a brush, and fabrics. NPA is also demonstrated to be a suitable structure for inkjet nano-patterning and replication systems using the property of LBL films to form thin conformal coatings. Furthermore, by locally altering the CA on the NPA, transparent LBL films can be used to create overt and covert images that can be simply revealed by the human breath. These techniques of a transferable nanostructure and LBL can be useful as platforms for potential cost-effective wearable electronics, biosensing, energy-storage systems, and anti-counterfeit industry.

Supporting Information

Supporting Information is available from the Wiley Online Library or from the author.

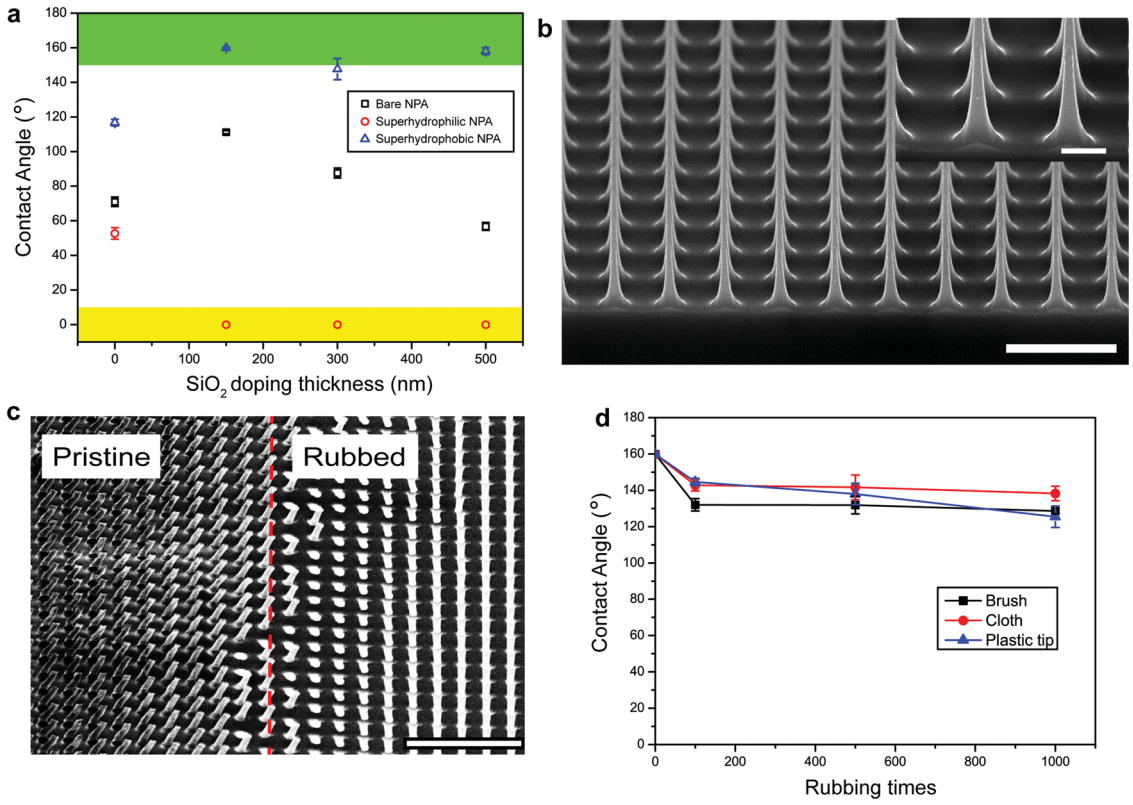

Figure 4. a) Overall CA changes corresponding to the different nanopillar structures and superhydrophobic (green region) and superhydrophilic (yellow region) coating. b,c) SEM images of pristine NPA (b) and after rubbing the NPA with a finger (c). The scale bars are 5 μm and 500 nm for the main and inserted images, respectively. d) CA change over repeated mechanical rubbing using different materials.

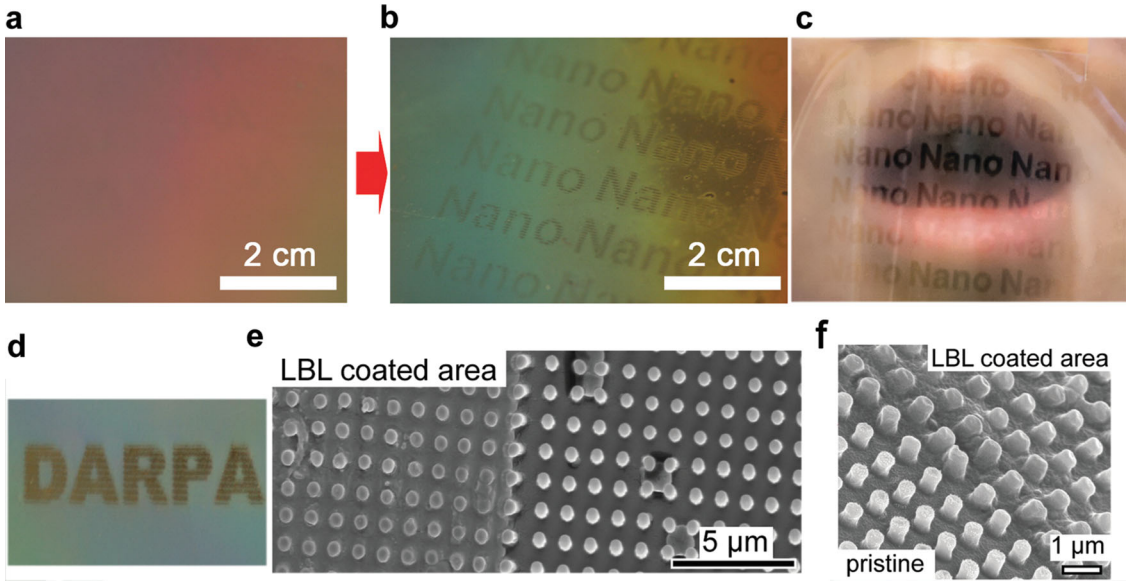

Figure 5. Hidden and overt images printed on nanopillar arrays using inkjet LBL deposition. Photograph of the NPA with hidden image a) before and b) after breathing on it. c) SEM image of the edge of the image demonstrating the difference between pristine and LBL-coated nanopillars. d) Photograph of a logo inkjet printed on the PUNO NPA. e) SEM of the nanopillar at the edge of the images letter in (d), demonstrating the difference between pristine and LBL-coated nanopillar area.

Acknowledgements

K. G. L., B. G. C., and B. I. K. are contributed equally to this work. This work was supported by BioNano Health-Guard Research Center funded by the Mininstry of Science, ICT & Future Planning (MSIP) of Korea as Global Frontier Project (Grant Number H-GUARD_2013M3A6B2078945). The work is also partially supported by DARPA Phase II research grant, U. S. Army Research Office under Grant Award W911NF-10-1-0518, AFOSR Grant Award MURI W911NF-12-1-0407 as well as NSF iCorp program with grant IIP 1358450. The authors also acknowledge past support of this research effort from NSF under grants ECS-0601345, CBET 0933384, CBET 0932823, and CBET 1036672.

Received: March 19, 2014
Revised: June 3, 2014
Published online: August 6, 2014

[1] S. H. Kang, B. Pokroy, L. Mahadevan, J. Aizenberg, *ACS Nano* **2010**, *4*, 6323.
[2] Z. Fan, R. Kapadia, P. W. Leu, X. Zhang, Y. Chueh, K. Takei, K. Yu, A. Jamshidi, A. A. Rathore, D. J. Ruebusch, M. Wu, A. Javey, *Nano Lett.* **2010**, *10*, 3823.
[3] N. Kaji, Y. Okamoto, M. Tokeshi, Y. Baba. *Chem. Soc. Rev.* **2010**, *19*, 948.
[4] Z. Fan, H. Razavi, J.-W. Do, A. Moriwaki, R. Ergen, Y.-L. Chueh, P. W. Leu, J. C. Ho, T. Takahashi, L. A. Reichertz, S. Neale, K. Yu, M. Wu, J. W. Ager, A. Javey, *Nat. Mater.* **2009**, *8*, 648.
[5] Z. L. Wang, J. Song, *Science* **2006**, *312*, 242.
[6] C. Xie, L. Hanson, Y. Cui, B. Cui, *Proc. Natl. Acad. Sci. USA* **2011**, *108*, 3894.
[7] H. Lee, B. P. Lee, P. B. Messersmith, *Nature* **2007**, *448*, 338.
[8] A. Sidorenko, T. Krupenkin, A. Taylor, P. Fratzl, J. Aizenberg, *Science* **2007**, *315*, 487.
[9] Y. Tanaka, K. Morishima, T. Shimizu, A. Kikuchi, M. Yamato, T. Okano, T. Kitamori, *Lab Chip* **2006**, *6*, 230.
[10] W. K. Cho, I. S. Choi, *Adv. Funct. Mater.* **2008**, *18*, 1089.
[11] H. E. Jeong, K. Y. Suh, *Nano Today* **2009**, *4*, 335.
[12] Y. Xia, G. M. Whitesides, *Annu. Rev. Mater. Sci.* **1998**, *28*, 153.
[13] S. H. Ahn, L. J. Guo, *ACS Nano* **2009**, *3*, 2304.
[14] P. Kim, W. E. Adorno-Martinez, M. Khan, J. Aizenberg, *Nat. Protoc.* **2012**, *7*, 311.
[15] W. L. Noorduin, A. Grinthal, V. Mahadevan, J. Aizenberg, *Science* **2013**, *340*, 832.
[16] B. Su, S. Wang, Y. Wu, X. Chen, Y. Song, L. Jiang, *Adv. Mater.* **2012**, *24*, 2780.
[17] M. D. Volder, A. J. Hart, *Angew. Chem. Int. Ed.* **2013**, *52*, 2412.
[18] Y. Kim, Z. Jian, B. Yeom, M. D. Prima, X. Su, J. G. Kim, S. J. Yoo, C. Uher, N. A. Kotov, *Nature* **2013**, *500*, 59.
[19] L.-S. Teo, C.-Y. Chen, J.-F. Kuo, *Macromolecules* **1997**, *30*, 1793.
[20] C. Pang, G. Y. Lee, T. Kim, S. M. Kim, H. N. Kim, S.-H. Ahn, K.-Y. Suh. *Nat. Mater.* **2012**, *11*, 795.
[21] A. Amirsadeghi, J. J. Lee, S. Park, *J. Micromech. Microeng.* **2011**, *21*, 115 013.
[22] D. B. Wolfe, J. C. Love, G. M. Whitesides, "*Nanostructures replicated by polymer molding" in Encyclopedia of Nanoscience and Nanotechnology,* Marcel Dekker, NJ, USA, **2004**.
[23] H.-W. Engels, *Angew. Chem. Int. Ed.* **2013**, *52*, 2.
[24] K. M. Choi, J. A. Rogers, *J. Am. Chem. Soc.* **2003**, *125*, 4060.
[25] J. Park, Y. S. Kim, T. Hammond, *Nano Lett.* **2005**, *5*, 1347.
[26] L. F. M. Da Silva, M. J. C. Q. Lopes, *Int. J. Adhes. Adhes.* **2009**, *29*, 509.
[27] J. B. Lambert, *Introduction to Organic Spectroscopy,* Macmillan, 1st ed., New York, NJ, USA **1987**.
[28] X. Deng, L. Mammen, H. J. Butt, D. Vollmer, *Science* **2012**, *335*, 67.
[29] C. Badre, T. Pauporté, M. Turmine, D. Lincot, *Nanotechnology* **2007**, *18*, 365 705.
[30] C. M. Andres, N. A. Kotov, *J. Am. Chem. Soc.* **2010**, *132*, 14 496.